Advances in Science and Technology Research Journal

Advances in Science and Technology Research Journal, 2026, 20(5), 503–520
https://doi.org/10.12913/22998624/217296
ISSN 2299-8624, License CC-BY 4.0

Received: 2025.12.05
Accepted: 2026.03.15
Published: 2026.04.01

Thermal performance enhancement of flat plate solar collectors using triangular tubes and nanofluids: A computational fluid dynamics approach

Diana Hassan Katea[1*], Iman Jabbar Awda[2]

[1] Energy Engineering department, University of Baghdad, Baghdad, Iraq
[2] Aeronautical Engineering Department, University of Baghdad, Baghdad, Iraq
* Corresponding author's e-mail: d.hassan1809@coeng.uobaghdad.edu.iq

ABSTRACT

Flat-plate solar collectors (FPSCs) are widely used in solar thermal applications, yet their efficiency is often hindered by conventional circular tube geometries and the limited thermal properties of water. This study introduced a novel approach by utilizing triangular-shaped riser tubes and nanofluids (Al_2O_3-water and CuO-water at 2% volume concentration). The simulation, conducted via computational fluid dynamics (CFD), focused on the climatic conditions of Baghdad, Iraq, during summer (June, July, August) and winter (January). The results demonstrate that triangular tubes enhance the effective heat transfer area and promote improved convective heat transfer characteristics. The CuO-water nanofluid achieved a maximum outlet temperature of approximately 423 K at a low flow velocity of 0.005 m/s. Furthermore, the combined use of triangular tube geometry and CuO-water nanofluid resulted in thermal efficiency improvements of up to 30–35%, compared to the conventional circular tubes operating with water under identical conditions.

Keywords: flat plate solar collector, triangular tubes, nanofluids, thermal efficiency, computational fluid dynamics, solar energy in Iraq.

INTRODUCTION

Solar energy stands as one of the most promising sustainable solutions to meet the escalating global energy demand [1, 2]. Among various solar thermal technologies, flat-plate solar collectors (FPSCs) are widely implemented due to their simple design and low maintenance costs [3, 4].

However, their thermal efficiency is inherently limited by two main factors: the conventional circular geometry of the riser tubes and the relatively poor thermophysical properties of water as a heat transfer medium [5]. Recent research has explored several techniques to overcome these limitations. For instance, the integration of nanofluids has shown significant potential in enhancing heat transfer coefficients [6]. Nanofluids, which are suspensions of metallic or non-metallic nanoparticles in a base fluid, exhibit superior thermal conductivity compared to pure water [7]. Furthermore, modifying the tube cross-section from circular to non-circular shapes, such as elliptical, can disrupt the thermal boundary layer and increase the contact surface area between the absorber plate and the fluid [8].

Despite the extensive literature on these enhancements [9, 10], there is a gap in the studies that simultaneously analyze the combined effect of triangular tube geometries and high-concentration nanofluids under the specific extreme solar irradiance levels found in Baghdad, Iraq. The transition from circular to triangular tubes is expected to induce secondary flow patterns that enhance mixing even in the laminar regime, which is a critical aspect often overlooked in standard designs.

Problem statement and objectives

The primary problem addressed in this work was the low heat extraction efficiency of conventional FPSCs during peak solar radiation periods in the regions with high ambient temperatures. Standard circular tubes often fail to maximize heat gain from the absorber plate due to limited contact area. Therefore, the objective of this study was to numerically investigate the thermal performance of a modified FPSC using triangular riser tubes combined with Al_2O_3-water and CuO-water nanofluids. Using a CFD-based approach, this paper evaluates the temperature distribution, outlet thermal gain, and overall efficiency for both circular and triangular geometries under the climatic conditions of Baghdad.

The study aimed to provide a robust design recommendation for enhancing solar thermal capture in high-temperature environments. Despite such developments, very little work has been carried out to explore the combined effects of tube geometry and the use of nanofluids in practical climatic conditions. In this regard, this work used CFD analysis for evaluating and optimizing the performance of flat plate solar collectors (FPSCs) integrated with triangular and circular tube geometries.

In this process, the three-dimensional model of the solar collector is developed in SolidWorks software and further solved in ANSYS Fluent software for carrying out the study. In this work, comparisons are made between the performance of water, Al_2O_3-water, and CuO-water nanofluids at 2% concentration and under similar conditions of operation, including the effects of solar radiation characteristic of the months of June, July, and August when solar radiation reaches its highest level during summer and also a study of the effect of performance during cold weather in winter, January. It may be expected that the observations made in the work can be of immense help in enhancing and optimizing the performance of FPSCs for solar heating applications.

MATERIALS AND METHODS

Geometrical model

The model system consisted of a flat-plate solar collector (FPSC) with a length and width of 1.0 m and 0.5 m, respectively. The absorber plate material was copper with a thickness of 2.5 mm, whereas the tubes had a wall thickness of 0.5 mm. In the absorber section, four tubes were set up in parallel, with a center-to-center space of 0.125 m. Figure 1 shows the geometrical configuration of the absorber tube contact in two ways: (a) in the case of circular tubes and (b) in the case of triangular tubes. The collector model includes an absorber plate integrated with riser tubes. Two configurations were analyzed: standard circular tubes and equilateral triangular tubes. The geometrical model explained above is summarized in Table 1.

Figure 2 (a–b) presents the three-dimensional geometrical models of the two designs. These models show the geometrical configuration of the solar collectors in the case of the circular tubes and the triangular tubes. FPSCs are a typical example of conventional solar collectors, which have the absorber plates located on top of cylindrical riser tubes. On the same note, the FPSC system contains triangular-shaped tubes as riser tubes that are directly installed on top of the absorber plates. This configuration allows for a higher contact

Table 1. The specifications of the geometrical model

Parameter	Value
Collector length	1.0 m
Collector width	0.5 m
Absorber plate thickness	2.5 mm
Tube material	Copper
Absorber plate material	Copper
Tube wall thickness	0.5 mm
Number of tubes	4
Tube shape	Circular / Triangular
Tube spacing	0.125 m

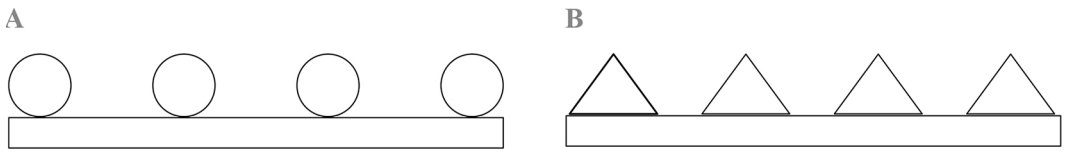

Figure 1. The engineering diagram of the contact between the plate and (a) the circular tube (b) the triangular tube

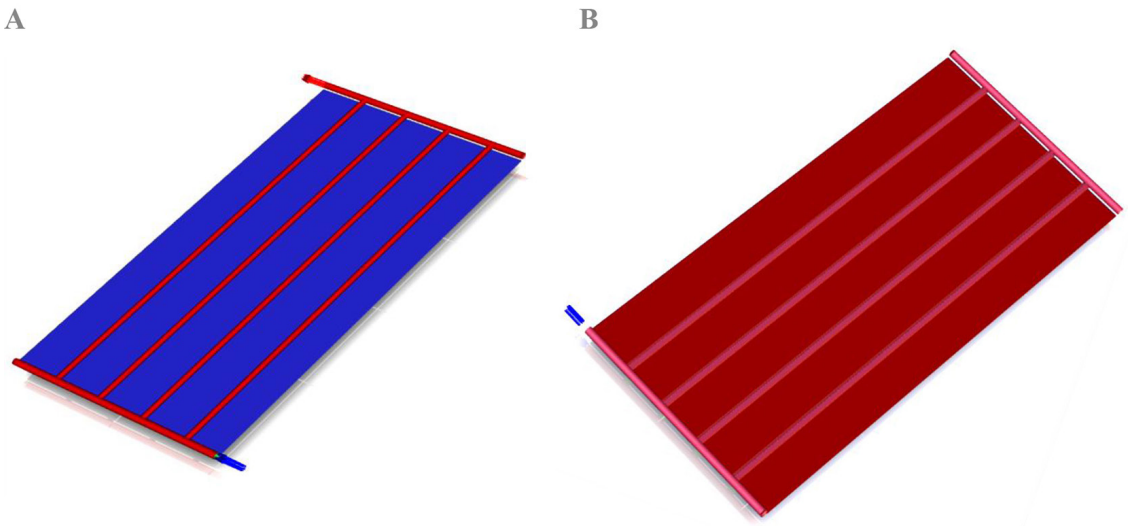

Figure 2. 3D geometrical model of the flat-plate solar collector with: (a) circular tubes, (b) triangular tubes

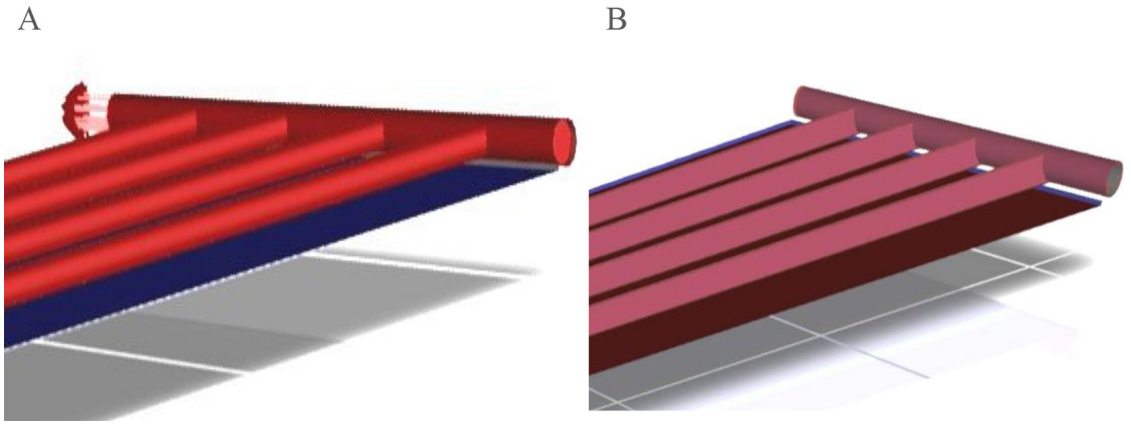

Figure 3. 3D geometrical configurations of the flat plate solar collector with (a) cylindrical riser tubes and (b) equilateral triangular riser tubes

surface between the absorber plates and the tubes, hence improving the flow of heat from the plates to the fluids.

Figure 3 shows three-dimensional geometrical configurations of the flat plate solar collector equipped with (a) circular tubes and (b) equilateral triangular tubes. The figure illustrates the tube arrangement beneath the absorber plate, as well as the inlet and outlet. Both tube geometries are designed to have equal cross-sectional area.

Fluid properties and nanoparticles

The working fluids used were pure water, CuO-water nanofluid, and Al_2O_3-water nanofluid with a 2% volumetric concentration of nanoparticles. The particles were assumed to be spherical and homogeneously distributed. The choice of a suitable heat transfer fluid for flat-plate solar collectors depends on the thermophysical properties of the fluid. These include thermal conductivity, viscosity, specific heat capacity, and freezing point, which determine the working temperature of the system. The following empirical correlations were used to determine the thermophysical properties of the nanofluids:

The density of the nanofluid (ρ_{nf}) was determined using the relation proposed by Pak and Cho (1998) [11]:

$$\rho_{nf} = (1-\phi)\rho_f + \phi\rho_p \quad (1)$$

where: (ρ_{nf}) density of the nanofluid (kg/m³), (ρ_f) density of the base fluid (kg/m³), (ρ_p) density of the nanoparticles (kg/m³) and (ϕ) nanoparticle volume fraction.

The specific heat capacity ($C_{p,nf}$) was calculated following Pak and Cho (1998):

$$C_{p,nf} = \frac{(1-\phi)\rho_f C_{p,f} + \phi\rho_p C_{p,p}}{\rho_{nf}} \quad (2)$$

where: ($C_{p,nf}$) specific heat capacity of the nanofluid (J/kg·K), ($C_{p,f}$) specific heat capacity of the base fluid (J/kg·K), ($C_{p,p}$) specific heat capacity of the nanoparticles (J/kg·K), (ρ_{nf}) density of the nanofluid (kg/m³) and (ϕ) nanoparticle volume fraction.

The dynamic viscosity (μ_{nf}) was obtained from the Brinkman (1952) model [12]:

$$\mu_{nf} = \frac{\mu_f}{(1-\phi)^{2.5}} \quad (3)$$

where: (μ_{nf}) dynamic viscosity of the nanofluid (Pa·s), (μ_f) dynamic viscosity of the base fluid (Pa·s), (ϕ) nanoparticle volume fraction.

The thermal conductivity (k_{nf}) was estimated using the Maxwell (1881) equation for spherical particles [13]:

$$k_{nf} = k_f \cdot \frac{k_p + 2k_f - 2\phi(k_f - k_p)}{k_p + 2k_f + \phi(k_f - k_p)} \quad (4)$$

where: (k_{nf}) thermal conductivity of the nanofluid (W/m·K), (k_f) thermal conductivity of the base fluid (W/m·K), (k_p) thermal conductivity of the nanoparticles (W/m·K), (ϕ) nanoparticle volume fraction. The calculated thermophysical properties for the nanofluids used in the CFD simulations are presented in Table 2.

All thermophysical properties are evaluated at 25 °C based on correlations reported by Pak and Cho (1998). On the basis of the standard material data, the properties of the nanoparticles were assumed to be sphericalnanoparticle size (30–50 nm) and their stability (non-aggregation) at 2% concentration. The base fluid (water) properties were obtained at the average operating temperature of the collector, corresponding to the midpoint between the inlet and outlet temperatures.

The Reynolds number (Re) for all simulated cases was calculated based on the hydraulic diameter of both circular and triangular tubes. In all scenarios, Re remained below 2300 (ranging from Re 150 to 800), confirming that the flow regime is strictly laminar. The secondary vortices and enhanced mixing mentioned in the results are attributed to the geometric transitions and non-circular cross-sections, which induce Dean-like flow patterns, even at low Reynolds numbers.

Boundary conditions and assumptions

The boundary conditions were precisely defined to reflect realistic operating environments. A constant solar heat flux was applied to the top surface of the absorber plate. The effect of the inclination angle was neglected since a uniform heat flux was imposed on the absorber plate. The side and back walls of the collector were modeled with adiabatic boundary conditions to simplify the initial model, while convective and radiative heat losses to the surroundings from the top glass cover were accounted for using a combined heat transfer coefficient. The inlet flow was set as a 'Velocity Inlet' with a uniform temperature profile (T_{in}), and the outlet was defined as 'Pressure Outlet'. Standard initial conditions (T= 298 K) were applied to initialize the iterations.

- Inlet: Uniform velocity inlet with flow rates ranging from 0.005 to 0.055 m/s.
- Outlet: Pressure outlet at atmospheric pressure.
- Walls: No-slip condition for all the solid boundaries.
- Solar irradiance: Applied as uniform heat flux on the absorber plate: 911 W/m² (June), 900 W/m² (July), 937 W/m² (August) and 835 W/m² (January).

Table 2. Thermophysical properties of working fluids at ϕ = 2%

Fluid	Viscosity (Pa·s)	Density (kg/m³)	Thermal conductivity (W/m·K)	Specific heat (J/kg·k)
Water	0.000936 ±3%	997 ±1%	0.613 ±5%	4179 ±2%
CuO-Water	0.000936 ±5%	1106.06 ±1%	0.649 ±7%	3754.7 ±2%
Al_2O_3-Water	0.000936 ±5%	1056.46 ±1%	0.649 ±7%	3921.7 ±2%

The inlet temperatures were 313 K (June), 317 K (July), 314 K (August) and 287 K (January).

- Thermal losses: Convective and radiative heat losses from the glass cover were accounted for. Side and back surfaces were modeled as adiabatic.
- Flow regime: Calculations showed that the Reynolds number (Re) remains below 2300 for all cases, justifying a Steady-state Laminar flow model.
- Junction: The thermal contact between the triangular tubes and the absorber plate was modeled to reflect realistic heat conduction.

Governing equations

- The CFD simulations are based on the following assumptions:
- Steady-state, incompressible, and laminar flow.
- Negligible radiation and natural convection effects.
- Uniform solar heat flux applied on the absorber plate surface.

The governing equations are as follows:
Continuity equation [14]:

$$\nabla \cdot V = 0 \tag{5}$$

Momentum equation [15]:

$$\rho(V \cdot \nabla V) = -\nabla p + \mu \nabla^2 V \tag{6}$$

Energy equation [16] :

$$\rho c_p (V \cdot \nabla T) = k \nabla^2 T + S_T \tag{7}$$

where: ρ is the density, V is the velocity vector, p is the pressure, μ is the dynamic viscosity, c_p is the specific heat capacity, k is the thermal conductivity, T is the temperature, and S_T is the volumetric heat source term due to absorbed solar energy.

Numerical setup

These simulations were computationally done using ANSYS Fluent 2022 R2. The coupling of velocity and pressure was carried out by using the SIMPLE algorithm. The momentum and energy equations applied second-order upwind discretization for more accuracy.

GRID INDEPENDENCE AND VALIDATION

Grid independence test

A mesh sensitivity study was conducted using four levels of refinement. A grid independence study was conducted to ensure the accuracy of the numerical results. Four different mesh densities were tested. The variation in the outlet temperature (T_{out}) was monitored, taking the finest mesh as the reference case. The coarsest mesh showed a significant deviation, whereas the difference between the medium and the finest mesh was less than 0.5%, justifying the selection of the third mesh density for the subsequent simulations.

A grid independence study was carried out to investigate the impact of the number of grid elements on the stability of the output temperatures from the data. The study found that temperatures converged, with the percentage of variation declining from 0.55% to less than 0.03% once the number of grid elements exceeded 1.5 million, indicating stability. Thus, this number of grid elements is acceptable for achieving numerical stability and obtaining a solution without additional computation time. Table 3 presents the trend of values with percentage change for the various numbers of elements tested; in turn, Figure 4 shows the stability of the result with respect to the number of elements.

Validation

To validate the numerical model, results for the circular tube geometry were first compared with the experimental data of [17]. Furthermore, the nanofluid model was validated against the CFD results of [18], showing a maximum deviation of 4%. Although specific experimental data for the triangular tube geometry is limited in literature, the consistent performance of the current model across standard cases provides confidence in its predictive capabilities for the new geometries.

Table 3. Grid independence test result and variations

Number of elements	T_o (K)	Variation (%) in T_o
250,646	344.1	_
510,649	346	0.55
1,543,872	346.1	0.03
2,937,646	346.2	0.03
4,378,902	346.1	0.03

Figure 4 presents the comparison of outlet temperature and temperature difference (T_{out}–T_{in}) at high inlet temperature conditions, while Figure 5 shows the same parameters at low inlet temperature conditions. Figure 5a provides the relationship between temperature difference, ΔT, at high inlet temperature for both the CFD simulation and reference data. Both CFD and reference data are decreasing as the velocity flow rate increases, with the trend showing that a higher velocity flow will remove more heat. From the figures, it is clear that the CFD model is giving similar outlet temperature values as in Figure 5b, at high inlet temperature, matching the general decreasing trend as velocity flow rate increases. The results from the CFD simulations match closely with the reference data for high inlet temperature, with a maximum deviation of less than 5%. The numerical results were validated against experimental data for circular tubes. A minor deviation of approx. 1K was observed, which is within the acceptable range for numerical simulations and is attributed to the variations in environmental loss coefficients.

The following is the case for similar trends at low inlet temperatures. The correlation of temperature difference, ΔT, at low inlet temperature for different velocity flow rates (0.0015–0.0053 m/s) is shown in Figure 6a, the comparison of outlet temperature, as presented in Figure 6b, continues to show a strong correlation between CFD prediction and reference for low inlet temperature cases. The CFD prediction maintains a good correspondence with reference data, showing a satisfactory level of precision and validating that the model is functioning well.

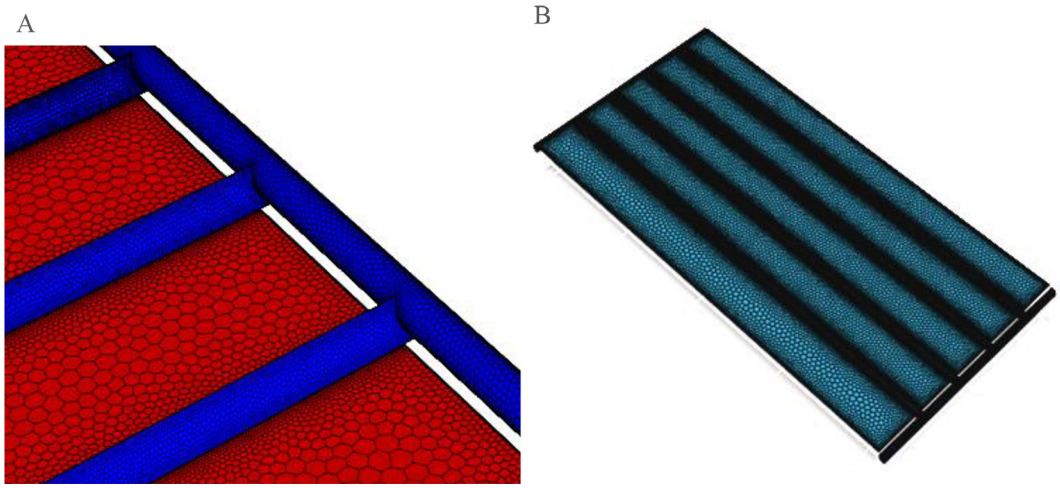

Figure 4. (a) Close-up of the mesh (b) mesh layout of the computational model

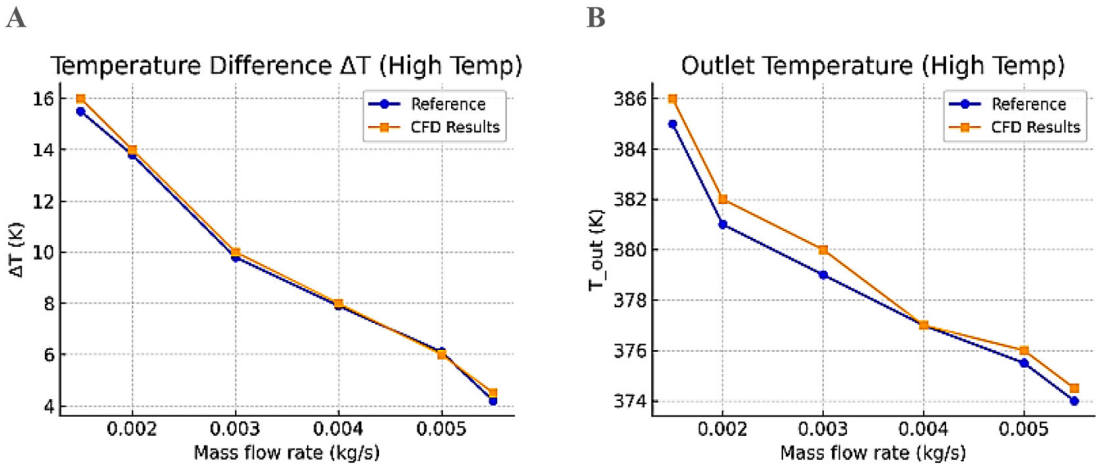

Figure 5. (a)Temperature difference (ΔT) at high inlet temperature (CFD vs Reference), (b) outlet temperature at high inlet temperature

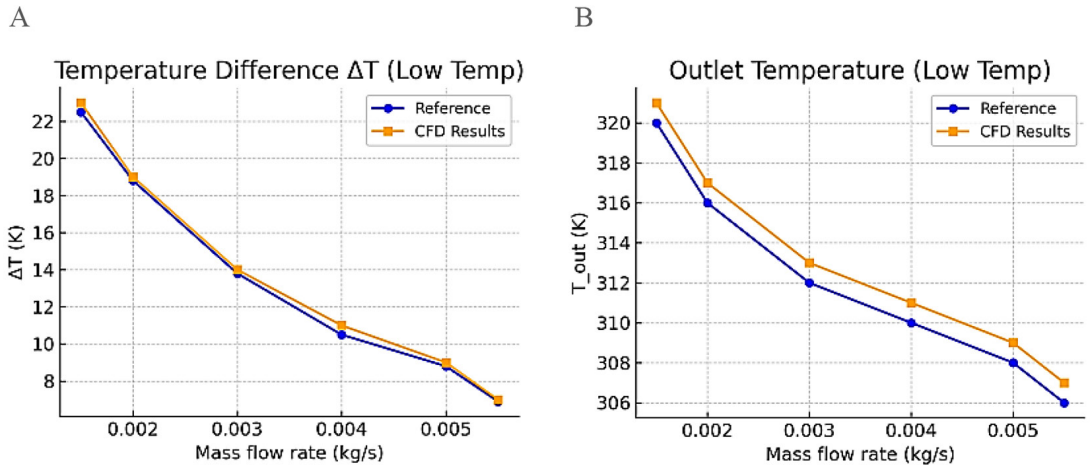

Figure 6. (a)Temperature difference (ΔT) at low inlet temperature (CFD vs Reference), (b) outlet temperature at low inlet temperature

RESULTS AND DISCUSSION

This section evaluated the results of the solar collector system analysis, with a focus on how absorber shape (triangular vs. circular), working fluids, and other factors affect performance. (water, Al_2O_3-water, and CuO-water nanofluids), and velocity flow rate, supported with figures, and compared with existing literature.

Thermal efficiency and flow rate

The trends in thermal efficiency (η) of the Flat Plate Solar Collector (FPSC) with velocity flow rate for both tube geometries (circular and triangular) as well as the aforementioned working fluids, i.e., water, CuO-water, and Al_2O_3-water nanofluids. As it can be noted in Figure 7, thermal efficiency showed an increasing trend coinciding with the velocity flow rate in all analyzed scenarios.

At lower flow rates (0.005 m/s), the efficiencies were found to range between 63–65% for triangular tubes and 60–62% for circular tubes under pure water utilization. Increasing the flow rate up to 0.025 m/s enhanced the efficiency up to around 81.9% for triangular tubes and around 78.5% for circular tubes under CuO-water nanofluid utilization. This trend can be attributed to increasing convective heat transfer coinciding with enhanced flow rates that cause a rise in desirable heat gain despite reducing the fluid residence time.

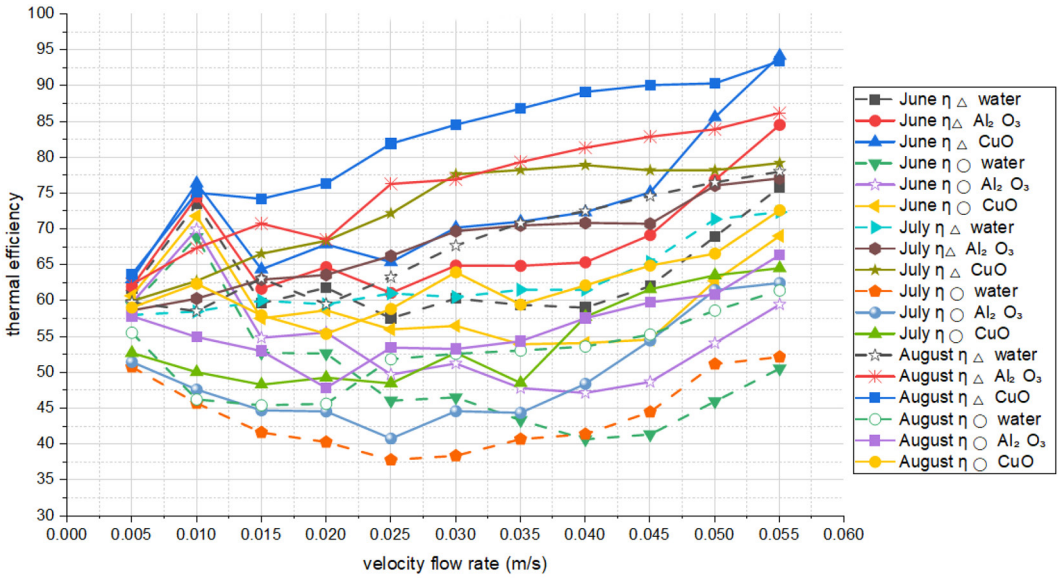

Figure 7. Thermal efficiency of triangular and circular absorbers with different working fluids

The effect on collector efficiency by nanofluid type is compared in Figure 6, CuO-water nanofluid maintained the largest enhancement in efficiency with gains up to 7.2% over water, as against an intermediate gain (~4.6%) by Al_2O_3-water nanofluid. The triangular geometry enhanced this effect further, with the highest efficiency realized under all velocity flow rates. Triangular channels improve mixing as well as convective behavior on enhanced collection by nanofuids [19, 20].

These results illustrate the dual advantage of geometrical optimization (triangular tubes) and enhanced working fluids (CuO-water nanofluid) in enhancing FPSC performance. The rise in efficiency as found here agrees with the local experimental findings as well as CFD prediction on an international level, validating the validity of the current numerical model [5].

FPSC showed the lowest value of thermal efficiency in the month of January, and this could be related to the reduced solar irradiance and lower values of inlet temperatures, while the value of flow velocity showed an equal increase. Even with the use of CuO-water nanofluid and triangular tubing, the maximum value of efficiency could not exceed 40–41%, which is substantially lower compared to the summer results. A detailed analysis of the collector's performance during January was provided separately in the Monthly Analysis section.

Monthly performance (June-July-August)

Variation of thermal efficiency. With the increase in velocity from 0.005 to 0.015 m/s, there was an increase in thermal efficiency along with the decrease in the exit temperature due to lower residence times. In addition to that, triangular-shaped tubes showed an increase in efficiency up to approximately 25% in comparison to the circular tube with CuO-water nanofluids at higher flow rates.

June performance

Figures 8 and 9 illustrate the thermal efficiency and outlet temperature behavior of a flat-plate solar collector in June at an inlet temperature of 313 K and a constant heat flux of 911 W/m² for triangular and circular tube cross-sections using water, Al_2O_3-water nanofluids, and CuO-water. The results show that thermal efficiency increases significantly along with flow velocity in all cases. For example, the efficiency of the triangular tube collector using CuO-water nanofluid increased from approximately 63% at 0.005 m/s to approximately 94–95% at 0.055 m/s, while the efficiency of the water in the triangular tubes increased from approximately 61% to 76% within the same velocity range. In contrast, the circular tubes recorded lower values, with the efficiency of the water at 0.055 m/s reaching only about 50%, compared to approximately 76% for the

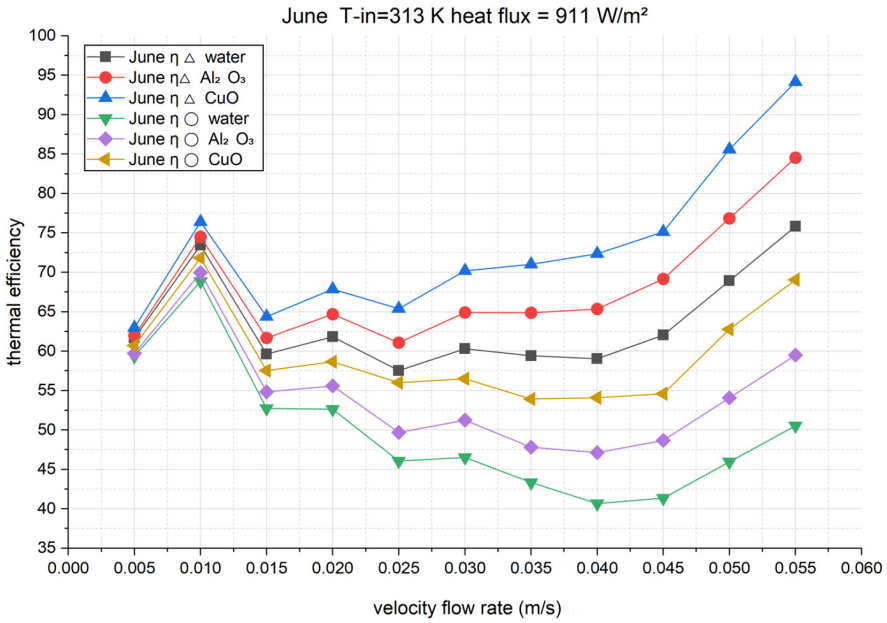

Figure 8. Thermal efficiency variation with flow rate for June

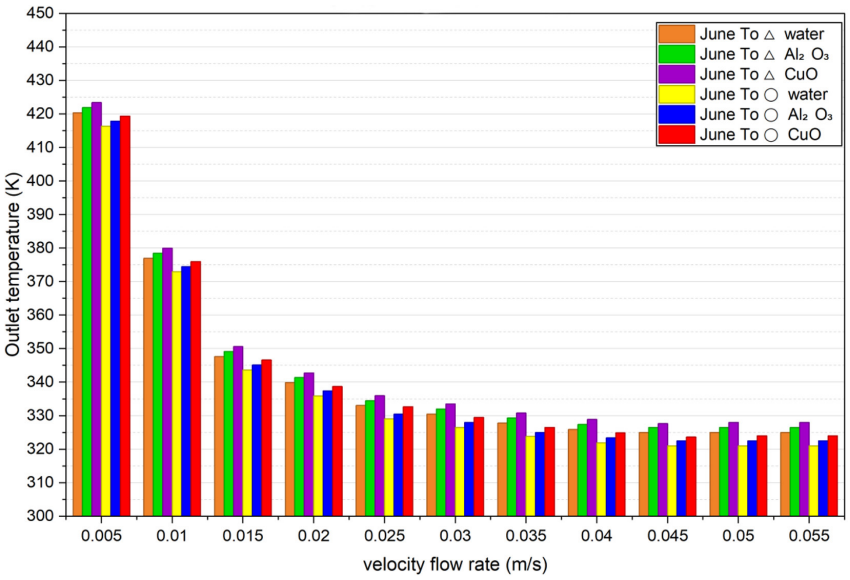

Figure 9. Outlet temperature variation with flow rate for June

triangular tube, representing an improvement of approximately 26 percentage points in favor of the triangular geometry.

At a velocity of 0.05 m/s, the triangular tubes achieved a similar improvement for all fluids, amounting to approximately 23 °C compared to the circular tubes for water, Al_2O_3-water, and CuO-water. This confirms the positive effect of the tube geometry on enhancing heat transfer due to the increased conducted area and the surrounding area ratio. Furthermore, CuO-water nanofluids exhibited the highest thermal performance compared to Al_2O_3-water and water. At a velocity of 0.03 m/s in the triangular tubes, the thermal efficiency of water was approximately 60%, rising to 65% with Al_2O_3-water and then to approximately 70% with CuO-water – a relative increase of approximately 15–17% compared to water.

With regard to the outlet temperature, when the flow velocity was increased, the outlet temperature decreased, as shown by the outlet temperature measurements on the CuO-water nanofluid flowing through the triangular tube. The outlet temperature of the CuO-water nanofluid flowing through the triangular tube decreased from approximately 423 K at 0.005 m/s to approximately 328 K at 0.055 m/s. Because the triangular tube had a higher outlet temperature than the circular tube at the same flow velocity and fluid type (i.e., 3 to 4 K), this implies the superior capacity for heat absorption and transfer of the triangular tube. Therefore, based on the study of the summer operating conditions, the combination of the triangular tube with the CuO-water nanofluid will result in the highest thermal performance of the flat-plate solar collector.

July performance

In July, the thermal performance and outlet temperature trends of a flat-plate solar collector at an inlet temperature of 317 K and constant heat flux of 900 W/m² were reported based on the performance of triangular tube sections and circular tube sections, as shown in Figures 10 and 11 with water, Al_2O_3-water, and CuO-water nanofluids. The study found that the thermal performance improved with increasing flow velocities for all fluid types. The thermal performance of CuO-water in triangular tubes was 60% at 0.005 m/s, while it improved to approximately 79 or 80% with the increase in flow velocity to a range between 0.055 m/s. Water performance in triangular tubes was 58% and improved to approximately 72% as flow velocity increased to 0.055 m/s. The circular tubes were found to perform significantly worse than their triangular counterparts, where the water performance was approximately 52% at 0.055 m/s. In comparison, the water performance in triangular tubes was approximately 72%, approximately a 20% performance gain with the triangular geometry compared with the circular geometry. The triangular tube performance with the average flow rate of 0.03 m/s was approximately 61% for water, 70% for the Al_2O_3-water nanofluids, and 78% for the CuO-water nanofluids. In

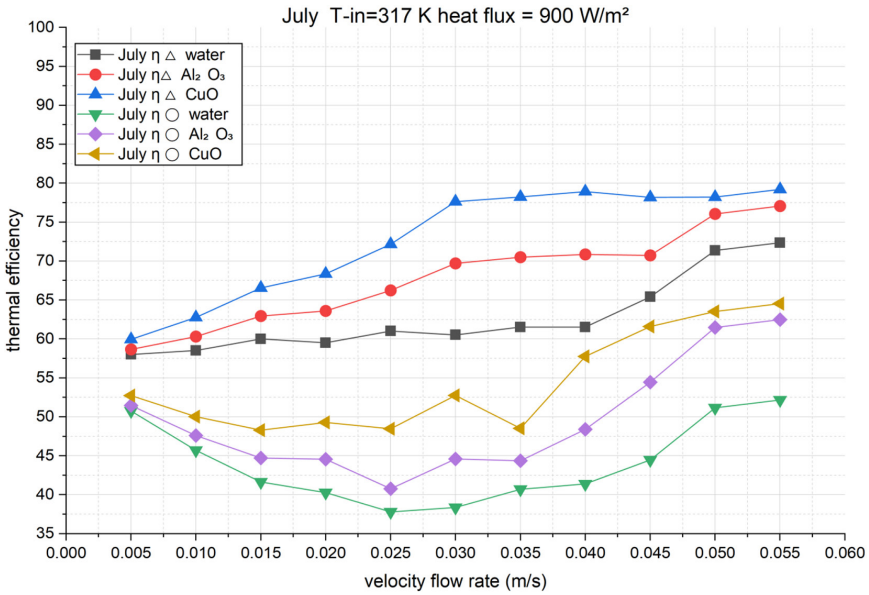

Figure 10. Thermal Efficiency variation with flow rate for July

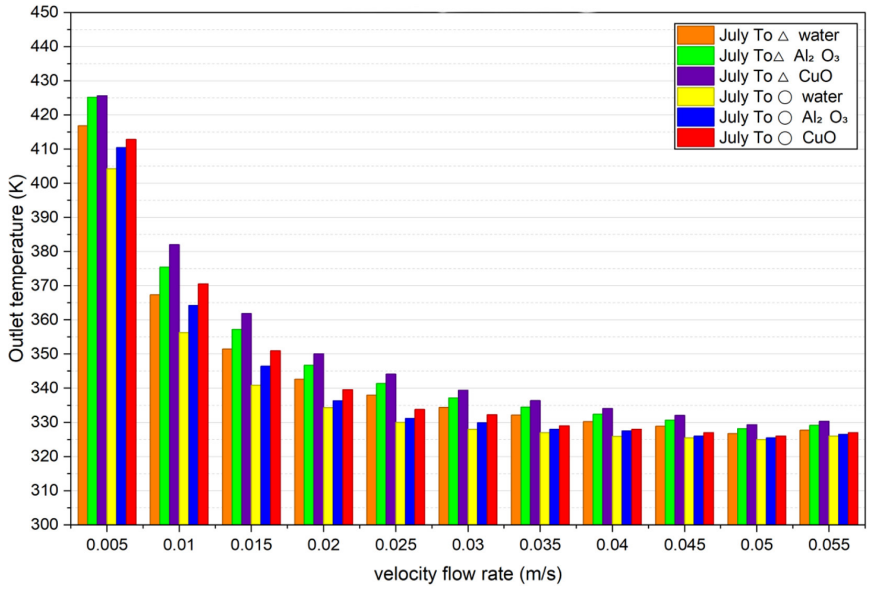

Figure 11. Outlet temperature variation with flow rate for July

comparison, the performance of circular tubes was 38%, 45%, and 53% for water, Al_2O_3-water, and CuO-water, respectively, indicating that the performance gain was between 40% and 60% due to the change in tube geometry. The use of nanofluids versus water clearly demonstrated improved thermal performance. The Al_2O_3-water nanofluids improved thermal efficiency approximately 10% to 12%, while the CuO-water nanofluids improved thermal efficiency by approximately 18% to 20% compared with water at the same flow rate and that affect also had been observed in [21].

The outlet temperature exhibited a marked decline with increasing flow rates. With a calculated exit point temperature beginning at roughly 425 K using a 0.005 m/s flow rate, the CuO-water nanofluid flowing through triangular-shaped tubing experienced a drop in exit point temperature down to around 330 K using a 0.055 m/s flow rate (both representing a 95 K reduction for shorter residence time periods). In addition, for the same velocity and fluid type, exit point temperatures were consistently higher (3–6 K) when using triangular-shaped tubing than when using circular-shaped tubing, which

indicates a superior transfer and absorption efficiency from the solar collector to the fluid. The results of these tests demonstrate that the optimal combination of the CuO-water nanofluid and triangular-shaped tubing provides superior thermal performance for FPSCs under summer (July) operating conditions.

August performance

For FPSC efficiency and outlet temperature, Figures 12 and 13 show monthly averages for August with a 314 K inlet and a 937 W/m² heat flux for triangular and circular tube-shaped sections filled with water, the Al_2O_3-water nanofluids, or CuO-water nanofluids. The data shows that for all cases where flow velocity was increased, thermal collector efficiencies improved. In the case of the CuO-water nanofluids in triangular tube sections, efficiencies increased from about 64% at 0.005 m/s to approximately 93–94% at 0.055 m/s, which equates to approximately a 29–30% increase. Comparatively, the improvement in efficiency for water in triangular tube sections at the same flow velocities was only around 18–20%. The performance of circular tubes was considerably lower, with a maximum efficiency of approximately 61% at 0.055 m/s for high-conductivity

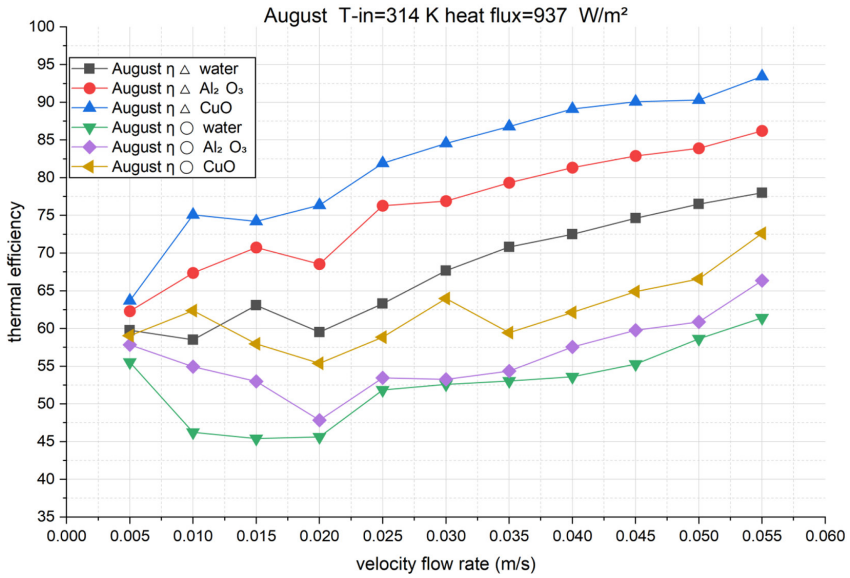

Figure 12. Thermal efficiency variation with flow rate for August

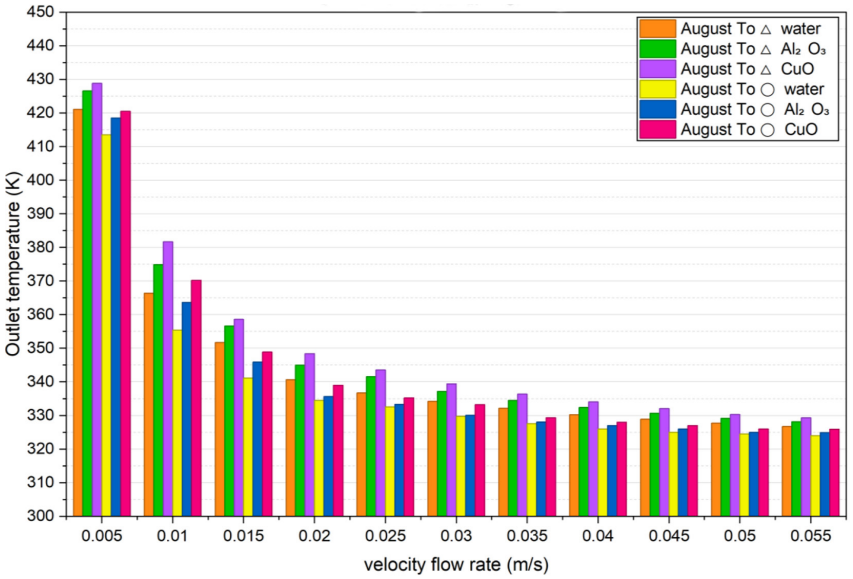

Figure 13. Outlet temperature variation with flow rate for August

fluids, while triangular tubes reached 78% at this flow; therefore, improving thermal efficiencies by about 17% due to better geometric design. The average velocity of 0.03 m/s increased the thermal efficiencies of triangular tubes to 68% for water, 77% for the Al_2O_3-water nanofluid, and 85% for the CuO-water nanofluid, whereas the circular tubes did not reach an efficiency higher than 52%, 53%, and 64%, respectively as performance analysis of solar thermal.

Therefore, the more effective triangular design provides an approximate 30–40% lift to thermal collector overall performance. The comparative performance of triangular versus circular tubes is quite clear when considering the effect of fluid type; in the case of the Al_2O_3-water nanofluid, efficiencies increased by approximately 10–12% against the water baseline, whereas the CuO-water nanofluid yielded an increase of approximately 20–22% over the water baseline when both fluids are pumped at the same velocities.

The decrease in outlet temperature was due to the shorter residence time associated with the increasing flow velocity. With respect to the exit temperature of the CuO-water nanofluid flowing through the triangular tubes, the maximum exit temperature at a flow velocity of 0.005 m/s was about 429 K, whereas the minimum exit temperature at a flow velocity of 0.055 m/s was approximately 330 K; thus, this represents a temperature drop of approximately 99 K.

The exit temperatures of the CuO-water nanofluid in the triangular tubes were higher than those of the CuO-water nanofluid in the circular tubes by 4 to 6 K for the same flow velocity and fluid type, indicating that the triangular tubes were more efficient than the circular tubes in terms of heat absorption and transfer efficiency. From these results, it can be concluded that, due to the total irradiance of 4.5 kWh/m²/day, August experiences the best thermal performance, especially with respect to the use of the CuO-water nanofluid also found that increasing the flow rate and the nanoparticles leads to a clear improvement in heat transfer.

January performance

Figures 14 and 15 show the thermal efficiency and outlet temperature of the flat-plate solar collector in the month of January, with a low heat flux of 835 W/m², a temperature of 287 K, and a solar irradiance that is lower compared to the summer months. Even with the lower absolute thermal efficiency in the month of January compared to the summer months, the graphs show that the triangular-shaped tubes and the use of nanofluids, specifically CuO-water, significantly improve the thermal performance capabilities of the solar collector in the winter months. With regard to the thermal efficiency, the data shows that the efficiency ratio increases along with velocity, reaching a point where it slightly drops with the increase in the velocity. The peak thermal efficiency for the CuO-water nanofluid in the triangular-shaped tubes reaches about 40–41% at a velocity of about 0.04 m/s,

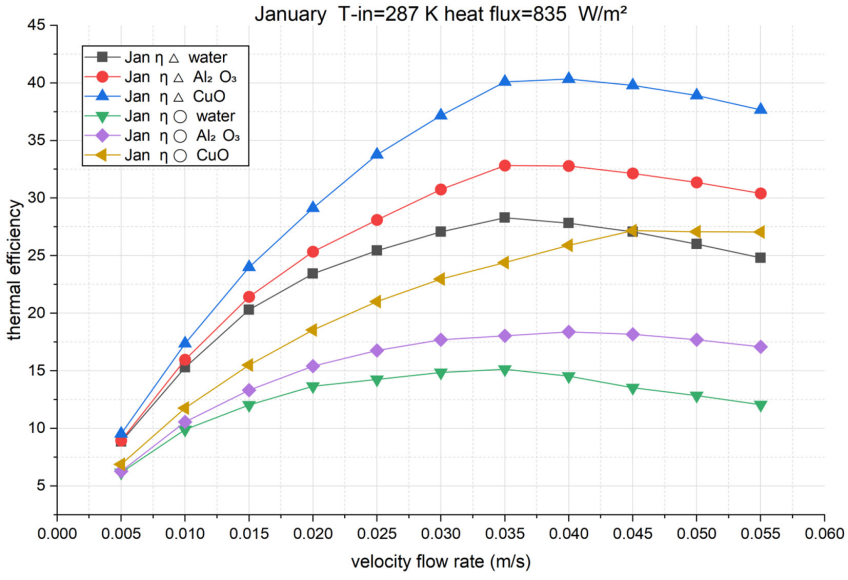

Figure 14. Thermal efficiency variation with flow rate for January

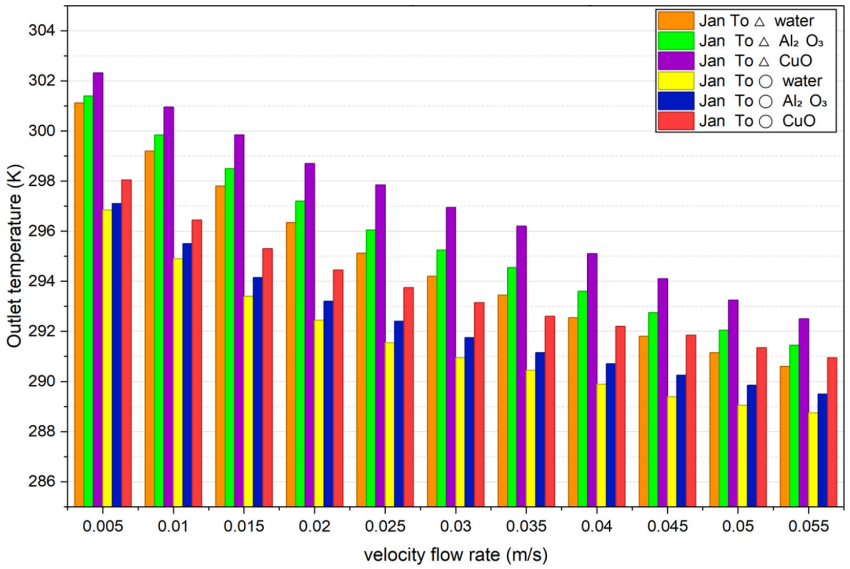

Figure 15. Outlet temperature variation with flow rate for January

compared to the approximately 28% in water and the 33% in the Al_2O_3-water nanofluid.

However, the peak thermal efficiency for the CuO-water nanofluid in the circular-shaped tubes did not exceed 27%, with the lowest thermal performance being that of the water, which reached a peak of about 15%. This shows that the use of the triangular-shaped tubes with the CuO-water nanofluid has a thermal performance increase that is above 45–50% compared to the use of the solar collector in the circular-shaped tubes.

It is clear that the value of the outlet temperature reduces linearly with the augmentation in the value of the flow velocity for all cases, owing to the shorter residence times in the tubes. For example, for CuO-water nanofluid in triangular sections, the value of the outlet temperature reduces from about 302 K at 0.005 m/s to about 292.5 K at 0.055 m/s, representing a decrease of about 9.5 K. In contrast, the values of the outlet temperatures for circular sections are lower, and the difference in the values for triangular and circular sections varies from 2 to 4 K for the same values of the flow velocity and fluids.

Summary of monthly trends

The seasonal analysis indicated that:

- January recorded the lowest thermal performance due to the lower solar heat flux of about 835 W/m², with the highest efficiency limited to 40–41%.
- In June and July, there were remarkable improvements in efficiency of around 95% and 80%, respectively, in CuO-water nanofluid in triangular tubes.
- The maximum performance in terms of overall efficiency was noted by August when the maximum solar irradiance measured about 937 W/m², with an efficiency close to 93–94% and an outlet temperature in excess of 420 K.
- For all months, the triangular tubes showed a steady improvement over the circular tubes of up to 15–35%.
- The CuO-water nanofluid had a better thermal performance compared to the Al_2O_3-water nanofluid and water.

Thermal distribution contours

Figures 16–22 illustrate the thermal profiles of the working media inside both the circular and the triangular channels for different velocity flow rates.

Effect of channel geometry: triangle vs. circular

Analysis has also shown that the cross-sectional shape of the tubes fixed on the absorber plate has been found to have a direct influence on the performance characteristics of the solar collector. As indicated in Figure 16, the non-uniform temperature distributions generated by the triangular tubes included concentrated hot regions around the corners. Triangular tubes have been found to have better thermal performance due to increased convection and mixing inside the tubes, while round tubes provide better thermal

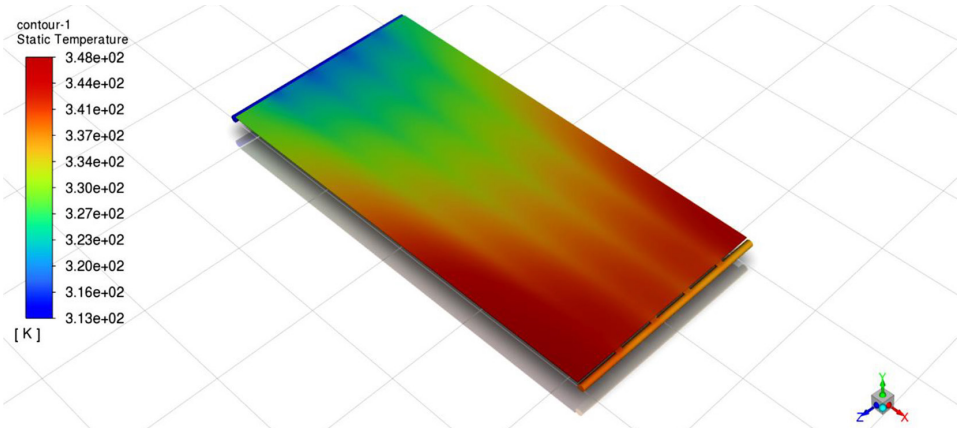

Figure 16. Temperature contour of triangular cross-section tubes

distribution with less pressure loss. Therefore, the use of triangular tubes is recommended when high thermal performance is required, while round tubes should be considered when high hydraulic stability is essential [22].

This is a representation shown in Figure 17, of the uniform convection heat transfer of round tubes. The round nature of these tubes enables a uniform flow of fluid along the inner surface of the tube, thus reducing hot spots on the plate. However, the pressure drop of round tubes is lower compared to other configurations.

Effect of working fluid

In Figure 18, the temperature distribution in the absorber surface for pure water as the working fluid is shown. The temperature

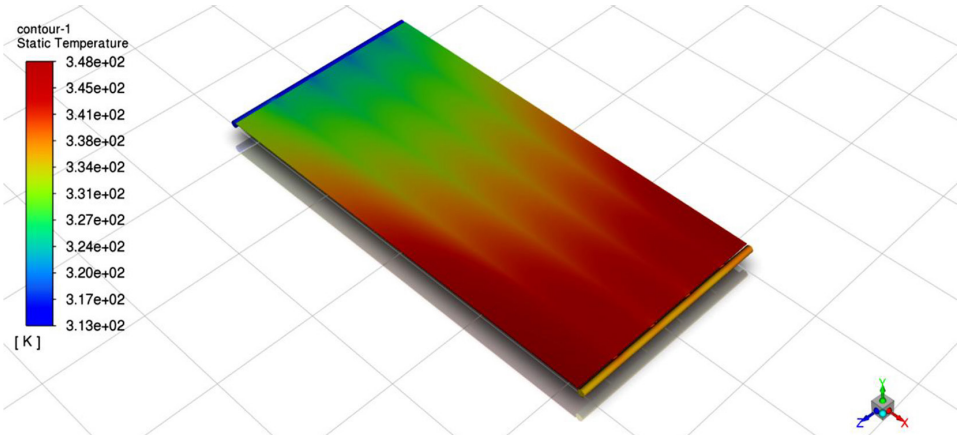

Figure 17. Temperature contour of circular cross-section tubes.

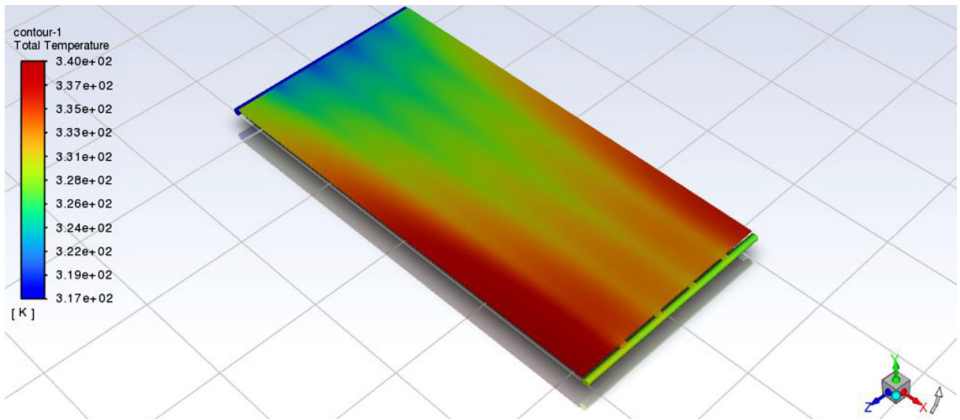

Figure 18. Total temperature distribution using pure water

increases from the inlet to the outlet with moderate values of maximum temperatures.

This indicates the absence of convective heat transfer, as the value of the thermal conductivity of the fluid is lower in the case of pure water compared to nanofluids. This indicates that the absorbed solar radiation is retained in the solar collector in the form of the absorber's internal energy, which is in accordance with the numerical analysis that states the poor performance of pure water in the flat-plate solar collector [23].

Figure 19 shows an improvement in the intensity and uniformity of the temperature distribution when the Al_2O_3-water nanofluid is used compared to water, with higher overall heat transfer rates. This is because the use of Al_2O_3 nanoparticles improves the overall thermal conductivity of the fluid, thus enhancing the convective heat transfer from the absorber to the fluid. This agrees with the work of [24], where the use of metal oxide nanofluids is seen to improve the performance of flat-plate solar collectors.

In Figure 20, the greatest thermal performance is shown, which is represented by the high values of temperature and the wider range of temperatures, especially in the outlet area, as well as the uniform distribution of temperatures along the absorber. This shows the thermal benefit of the CuO-water nanofluid, which can be considered to be due to the high thermal conductivity of the CuO-water nanofluid compared to the Al_2O_3-water and pure water nanofluids. This result confirms the supremacy of the CuO-water nanofluid and the significant impact of the enhancement of the properties of the working fluid on the efficiency of the solar collector.

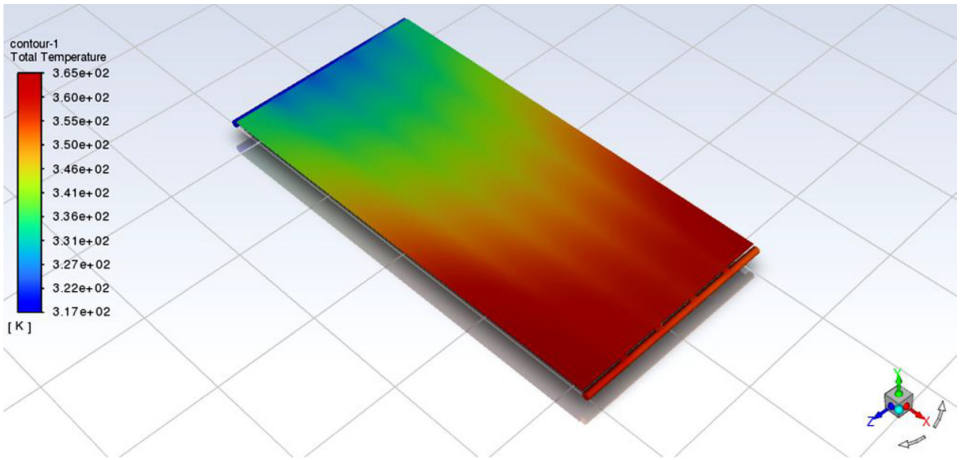

Figure 19. Total temperature distribution using the Al_2O_3–water nanofluid

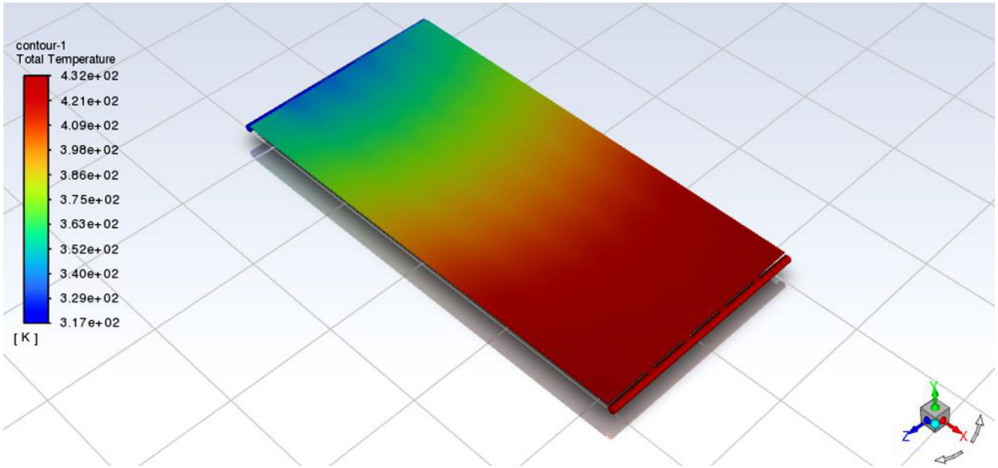

Figure 20. Total temperature distribution using CuO-water nanofluid

Effect of flow rate (velocity inlet)

The velocity of the working fluid is a basic parameter that determines the thermal efficiency of a solar collector. In Figure 21, at low velocities of the fluid (0.0005 m/s), the temperatures on the absorber plate surface vary significantly, ranging from 314 K at the end connected to tubes to 434 K at the other end of the solar collector. This large difference in temperatures on the absorber plate surface indicates low convective heat transfer between the absorber plate and the fluid inside the tubes due to low velocities of the fluid.

At low velocities, the convective heat transfer between the absorber plate and the fluid inside the tubes decreases, thereby increasing the accumulation of heat on the absorber plate surface, thus increasing the absorber plate temperature. This results in a decrease in the ability of the fluid to remove heat energy, thereby increasing the losses of heat energy to the surroundings. The increased accumulation of heat on the absorber plate surface increases the absorber plate temperature, thus decreasing the thermal efficiency of the solar collector [25, 26].

An increase in the flow speed to 0.015 m/s results in a significant enhancement of the temperature distribution over the absorber plate surface, which is restricted to the range of 314 K to 337 K, see Figure 22. This increase in flow speed significantly increases the convective heat transfer coefficient, thereby improving the heat transfer from the absorber plate surface to the fluid. Furthermore, the significant decrease in the absorber plate temperature indicates that the fluid is able to absorb more solar radiation, which is then converted to heat, thereby increasing the efficiency of the solar collector. Thus, determining the flow speed that increases the efficiency of the solar collector is essential [27].

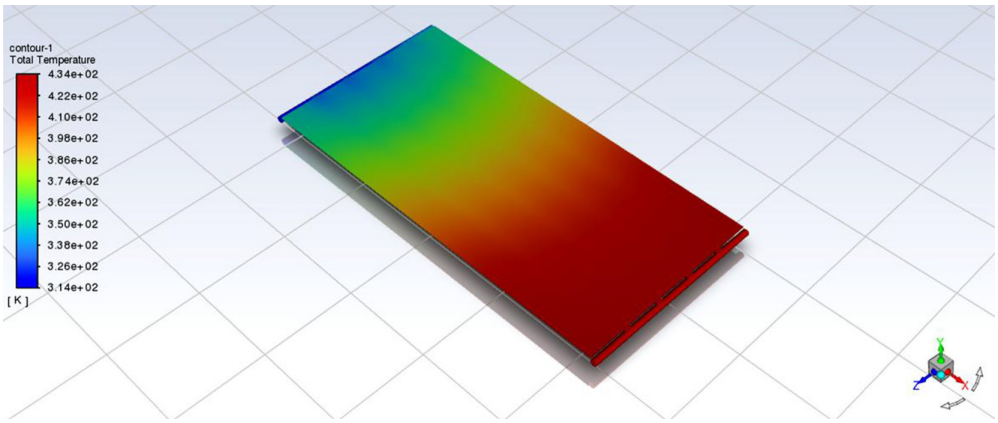

Figure 21. Temperature contour of triangular tube of CuO nanofluid at 0.0005 m/s

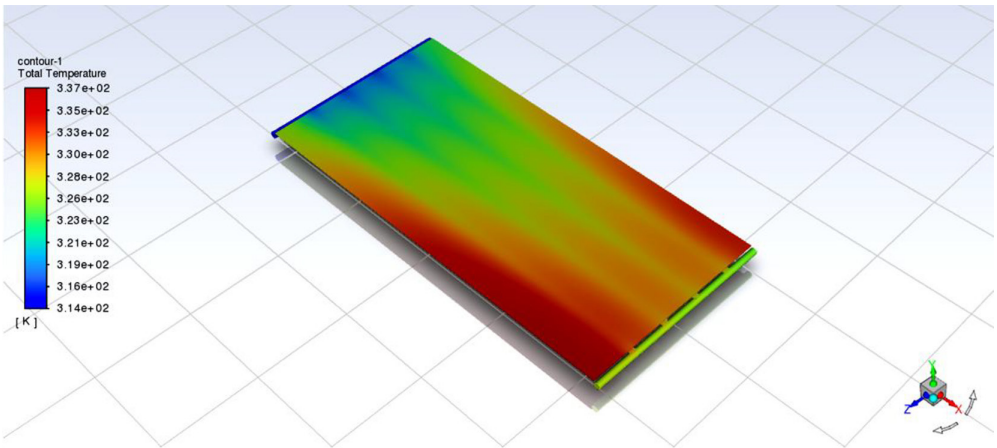

Figure 22. Temperature contour of triangular tube of the CuO nanofluid at 0.055m/s

CONCLUSIONS

This study reported on a comprehensive numerical study that analyzed the thermal performance of flat plate solar collectors (FPSCs) located in Baghdad utilizing both circular and triangular tubes with numerous working fluids. The data shows a strong influence on the collector's performance (efficiency and outlet temperature) from both the type of nanofluid used and the geometry of the tube. To summarize the major findings of this study:

- The thermal efficiency of the triangular tubes is always greater than that of circular tubes because of better heat transfer properties.
- Of the fluids tested, the CuO-water nanofluid performed the best, and the performance was followed by Al_2O_3-water and pure water.
- With the flow velocity of 0.005 m/s, the triangular tubes configuration of CuO-water gave the highest temperature of 423.4 K and efficiency of about 81.9%, indicating an improvement in efficiency of about 25–35% over the conventional configuration.
- The collector showed its highest efficiency in August, which is a result of the highest solar irradiance values, while January showed the lowest efficiency; however, the trend is uniform for all months.
- To conclude, the combination of the geometry of the triangular tube and the CuO-water nanofluid can be an effective approach for improving the FPSC performance.

REFERENCES

1. Al-Shamkhee, D., Alghurabe, M., Alsahlani, A. Experimental study of the performance of a flat plate solar water heater. In: 4th Scientific International Conference Najaf (SICN), 2019; 200–204. https://doi.org/10.1109/SICN47020.2019.9019371
2. Kadhim, S. A., Ibrahim, O. A. Improving the thermal efficiency of flat plate solar collector using nano-fluids as a working fluids: A review. Iraqi Journal of Industrial Research, 2021b; 8(3). https://doi.org/10.53523/ijoirvol8i3id86
3. Al-Kayiem, H. H., Mohammad, S. T. Potential of renewable energy resources with an emphasis on solar power in Iraq: An outlook. Resources, 2019; 8(1), 42. https://doi.org/10.3390/resources8010042
4. Ahmed, O. K. Effect of the dust on the performance of solar water collectors in Iraq. International Journal of Renewable Energy Development, 2016; 5(1), 65–72. https://doi.org/10.14710/ijred.5.1.65-72
5. Attia, O. H., Musawi, S. T. A., Mousa, N. A., Mahmood, H. A., Adam, N. M. Experimental evaluation of the performance of a domestic water heating system under Baghdad climate conditions. Eastern-European Journal of Enterprise Technologies, 2022; 6(8(120)), 38–47. https://doi.org/10.15587/1729-4061.2022.268026
6. Rostami, S., Hamid, A. S. A., Sopian, K., Jarimi, H., Bassim, A., Ibrahim, A. Heat transfer analysis of the flat plate solar thermal collectors with elliptical and circular serpentine tubes. Applied Sciences, 2022; 12(9), 4519. https://doi.org/10.3390/app12094519
7. Islam, R., Ali, M., Pratik, N., Lubaba, N., Miyara, A. Numerical analysis of a flat plate collector using different types of parallel tube geometry. AIP Advances. 2023. https://doi.org/10.1063/5.0159916
8. Genc, A. M., Ezan, M. A., Turgut, A. Thermal performance of a nanofluid-based flat plate solar collector: A transient numerical study. Applied Thermal Engineering, 2017b; 130, 395–407. https://doi.org/10.1016/j.applthermaleng.2017.10.16
9. Tang, X., Tan, C., Liu, Y., Sun, C., Xu, S. Numerical analysis on heat collecting performance of novel corrugated flat plate solar collector using nanofluids. Sustainability, 2024; 16(14), 5924. https://doi.org/10.3390/su16145924
10. Yakoub, N. G. Using hybrid nanofluids to improve the performance of flat plate solar hot water system. Journal of Advanced Engineering Trends, 2024; 43(2), 259–267. https://doi.org/10.21608/jaet.2023.201741.1243
11. Pak, B. C., Cho, Y. I. Hydrodynamic and heat transfer study of dispersed fluids with submicron metallic oxide particles. Experimental Heat Transfer, 1998; 11(2), 151–170. https://doi.org/10.1080/08916159808946559
12. Brinkman, H. C. The viscosity of concentrated suspensions and solutions. The Journal of Chemical Physics, 1952; 20(4), 571. https://doi.org/10.1063/1.1700493
13. Maxwell, J. C. A treatise on electricity and magnetism. Oxford, UK: Clarendon Press. 1881.
14. Çengel, Y. A., Cimbala, J. M. Fluid mechanics: Fundamentals and applications (3rd ed.). New York, NY: McGraw-Hill Education. 2014.
15. White, F. M. Fluid mechanics (7th ed.). New York, NY: McGraw-Hill Education. 2011.
16. Incropera, F. P., DeWitt, D. P., Bergman, T. L., Lavine, A. S. Fundamentals of heat and mass transfer (6th ed.). Hoboken, NJ: John Wiley & Sons. 2007.
17. Sahin, B., Manay, E., Akyurek, E. F. An experimental study on heat transfer and pressure drop of CUO-water nanofluid. Journal of Nanomaterials, 2015(1). https://doi.org/10.1155/2015/790839

18. Alobaid, M., Hughes, B., Heyes, A., O'Connor, D. Determining the effect of inlet flow conditions on the thermal efficiency of a flat plate solar collector. Fluids, 2018; 3(3), 67. https://doi.org/10.3390/fluids3030067
19. Verma, S. K., Tiwari, A. K., Tiwari, S., Chauhan, D. S. (2018). Performance analysis of hybrid nanofluids in flat plate solar collector as an advanced working fluid. Solar Energy, 167, 231–241. https://doi.org/10.1016/j.solener.2018.04.017
20. Hussein, A. M., Ali, H. H. M., Ali, Z. Assessing the efficacy of flat-plate solar collectors using nanofluids in the climatic context of Kirkuk city, Iraq. Acta Polytechnica, 2024; 64(1), 25–33. https://doi.org/10.14311/ap.2024.64.0025
21. Abid, M., Ratlamwala, T. H., Atikol, U. Performance assessment of parabolic dish and parabolic trough solar thermal power plant using nanofluids and molten salts. International Journal of Energy Research, 2015; 40(4), 550–563. https://doi.org/10.1002/er.3479
22. Elashmawy, M., Kolsi, L. Turbulent forced convection heat transfer in triangular cross sectioned helically coiled tube. International Journal of Advanced and Applied Sciences, 2016; 3(7), 18–23. https://doi.org/10.21833/ijaas.2016.07.004
23. Al-Waked, R., Al-Taie, A. M. Experimental and numerical investigation of heat transfer enhancement in a flat plate solar collector using nanofluids. Heat Transfer Engineering, 2020; 42(17–18), 1501–1515. https://doi.org/10.1080/08916152.2020.1847215
24. Hussein, A. M., Awad, A. T., Ali, H. H. M. Evaluation of the thermal efficiency of nanofluid flows in flat plate solar collector. Journal of Thermal Engineering, 2024; 10(2), 299–307. https://doi.org/10.18186/thermal.1448578
25. Al-Najjar, H. M. T. Study of energy gains by orientation of solar collectors in Baghdad City. Journal of Engineering, 2015; 21(10), 17–35. https://doi.org/10.31026/j.eng.2015.10.02
26. Jassim, N. A., Shbailat, S. J. Energy and exergy analysis of dual channel solar air collector with different absorber plates geometry. Journal of Engineering, 2018; 24(4), 19–40. https://doi.org/10.31026/j.eng.2018.04.02
27. Zeinali Heris, S., Oghazian, F., Khademi, M., Saeedi, E., Simulation of convective heat transfer and pressure drop in laminar flow of Al_2O_3/water and CuO/water nanofluids through square and triangular cross-sectional ducts. Journal of Renewable Energy and Environment, 2015; 2(1), 6–18.